Molecular Microbiology (2000) **37**(4), 740–751

Localization of components of the chemotaxis machinery of *Escherichia coli* using fluorescent protein fusions

Victor Sourjik and Howard C. Berg*
Department of Molecular and Cellular Biology, The Biological Laboratories, Harvard University, 16 Divinity Avenue, Cambridge, MA 02138, USA.

Summary

We prepared fusions of yellow fluorescent protein [the YFP variant of green fluorescent protein (GFP)] with the cytoplasmic chemotaxis proteins CheY, CheZ and CheA and the flagellar motor protein FliM, and studied their localization in wild-type and mutant cells of *Escherichia coli*. All but the CheA fusions were functional. The cytoplasmic proteins CheY, CheZ and CheA tended to cluster at the cell poles in a manner similar to that observed earlier for methyl-accepting chemotaxis proteins (MCPs), but only if MCPs were present. Co-localization of CheY and CheZ with MCPs was CheA dependent, and co-localization of CheA with MCPs was CheW dependent, as expected. Co-localization with MCPs was confirmed by immunofluorescence using an anti-MCP primary antibody. The motor protein FliM appeared as discrete spots on the sides of the cell. These were seen in wild-type cells and in a *fliN* mutant, but not in *flhC* or *fliG* mutants. Co-localization with flagellar structures was confirmed by immunofluorescence using an antihook primary antibody. Surprisingly, we did not observe co-localization of CheY with motors, even under conditions in which cells tumbled.

Introduction

Bacterial cells have a signal transduction pathway that allows them to sense and respond to changes in the concentrations of chemical attractants or repellents. In *Escherichia coli*, the addition of attractant or the removal of repellent promotes counterclockwise flagellar rotation or smooth swimming, which carries cells in a favourable direction. The signal transduction pathway includes a number of membrane-bound receptors, including four methyl-accepting chemotaxis proteins (MCPs: Tsr, Tar, Trg and Tap) and an oxygen receptor (Aer), six cytoplasmic chemotaxis proteins (CheA, CheW, CheR, CheB, CheY and CheZ) and three proteins comprising a switch complex at the cytoplasmic face of the flagellar motor (FliM, FliN and FliG). For reviews and recent structural work, see Bilwes *et al*. (1999), Djordjevic and Stock (1998), Falke *et al*. (1997), Kim *et al*. (1999) and Levit *et al*. (1998). The chemotactic signal is transmitted by autophosphorylation at His-48 of CheA, phosphoryl group transfer to Asp-57 of CheY (Hess *et al*., 1988a,b; Borkovich *et al*., 1989; Sanders *et al*., 1989) and binding of phosphorylated CheY to FliM (Welch *et al*., 1993), which stabilizes the clockwise and destabilizes the counterclockwise rotational states (Kuo and Koshland, 1989; Alon *et al*., 1998; Scharf *et al*., 1998). Dephosphorylation of CheY is accelerated by CheZ (Hess *et al*., 1988a).

The assembly of a ternary complex comprising MCP, CheW and CheA was shown to be necessary for CheA activation *in vitro* (Ninfa *et al*., 1991; Gegner *et al*., 1992), where it forms higher order structures (Liu *et al*., 1997). The formation of a quaternary complex, including CheY, has also been shown *in vitro* (Schuster *et al*., 1993). In addition, CheZ was found to interact with the short form of the histidine kinase, $CheA_S$ (Wang and Matsumura, 1996; 1997). Immunoelectron microscopy revealed that MCP–CheW–CheA complexes are clustered *in vivo*, predominantly at the cell poles (Maddock and Shapiro, 1993), but weaker lateral clusters also are observed (Lybarger and Maddock, 1999; Skidmore *et al*., 2000). CheA and CheW are required for strong clustering, but there is a significant level of CheA-independent clustering (Skidmore *et al*., 2000). Receptor clustering might be important for the generation of chemotactic signals (Bray *et al*., 1998; Levit *et al*., 1998; Duke and Bray, 1999).

The switch complex has been visualized by electron microscopy (Khan *et al*., 1992; Francis *et al*., 1994), in which it appears as a cytoplasmic ring (the C-ring) about 45 nm in diameter. The primary components of this ring are FliM and FliN. The remaining component of the switch complex, FliG, appears at the periphery of the MS-ring, where it forms a bridge to the C-ring. FliG is thought to be assembled first on the MS-ring, followed by the co-operative association of FliM and FliN (Zhao *et al*., 1995;

Accepted 31 May, 2000. *For correspondence. E-mail hberg@biosun.harvard.edu; Tel. (+1) 617 495 0924; Fax (+1) 617 496 1114.

Table 1. Functionality of YFP fusions.

Fusion protein	Functionality[a]	Presence of full-length product[b]
CheY–YFP	+ + +	+
YFP–CheY	+ +	+
CheZ–YFP	+ + + +	+
YFP–CheZ	+ + + +	+
YFP–$CheA_L$	–	+
YFP–$CheA_S$	ND	+
FliM–YFP	+ + + +	+
YFP–FliM	±[c]	+

a. Defined by complementation for spreading in soft agar (Fig. 1) as the ratio of the size of the outer swarm ring of the complementation strain to the size of the outer swarm ring of the wild-type strain, as follows: –, <0.15; ±, 0.15–0.3; + +, 0.4–0.5; + + +, 0.5–0.66; + + + +, >0.66.
b. Tested by immunoblot.
c. The YFP–FliM fusion complemented the *fliM* mutant for swimming in liquid media but only poorly for spreading in soft agar.

1996; Kubori *et al*., 1997; Khan *et al*., 1998): preparations of flagellar basal bodies that lack FliN also usually lack FliM, and vice versa. However, physical interactions among the three switch proteins, demonstrated both *in vitro* (Tang *et al*., 1996) and *in vivo* (Marykwas and Berg, 1996; Marykwas *et al*., 1996), suggest that FliM can interact with FliG by itself. Another contradiction is the observation by Oosawa *et al*. (1994), also made *in vitro*, that FliM can bind to the MS-ring in the absence of FliG.

Green fluorescent protein (GFP) and its mutants are now widely used to study the localization of proteins in living cells. For general reviews, see Conn (1999); for applications in bacteria, see Margolin (2000). A GFP fusion has already been used to study the localization of one of the chemotaxis proteins, CheZ (M. Manson, personal communication). This construct localizes to the cell poles to what appears to be MCP clusters, in apparent contradiction to the previous result that the interaction of CheZ with $CheA_S$ is blocked by the binding of $CheA_S$ to CheW (Wang and Matsumura, 1997).

In the present work, we used fusions to YFP (the S65G, V68L, S72A, T203Y GFP mutant) to study the localization in *E. coli* of the chemotaxis proteins CheY, CheZ and CheA, and the motor protein FliM. The chemotaxis proteins localized in a pattern of clusters in parallel with MCPs, as identified by immunofluorescence. This suggests the existence of a chemotaxis signal complex comprising five proteins: MCPs, CheW, CheA, CheY and CheZ. FliM–YFP localized to the flagellar motors, even in the absence of FliN, but not in the absence of FliG.

Results

YFP fusions to chemotaxis and motor proteins

In order to investigate the localization of chemotaxis and motor proteins in *E. coli* cells, we designed several fusions of YFP to the proteins CheY, CheZ, CheA and FliM, as summarized in Table 1. For CheY, CheZ and FliM, both C-terminal and N-terminal fusions were constructed. For CheA, two N-terminal fusions, YFP-$CheA_L$ and YFP-$CheA_S$, were constructed, corresponding to the long and short forms of the CheA protein (Kofoid and Parkinson, 1991). For all fusions, a short amino acid linker (3× or 5× glycine) was used (see *Experimental procedures*). The fusion genes were expressed under control of the arabinose promoter (pBAD), which allows tight regulation of expression (Guzman *et al*., 1995). The existence of full-length fusion proteins was verified by immunoblot (see *Experimental procedures*). YFP fusions to CheY, CheZ, CheA and FliM were tested for their ability to complement corresponding null mutants for spreading in soft agar (Fig. 1; Table 1). CheY, CheZ and FliM fusions complemented the null mutants in an inducer-dependent manner, suggesting that all these fusions are functional (although not as efficient as the wild-type proteins). However, the YFP–$CheA_L$ fusion did not complement the *cheA* null mutant. The induction level

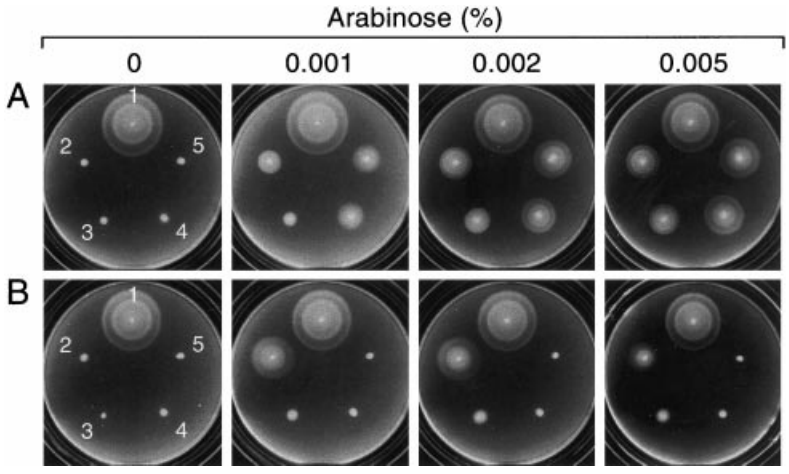

Fig. 1. Swarm plates illustrating the ability of different YFP fusion proteins to complement the corresponding null mutants. The concentration of arabinose (as a percentage), the inducer of gene expression for the pBAD constructs, is shown at the top.
A. Swarm ring formation by (1) RP437/pBAD18K wild type; (2) *cheY*/CheY–YFP; (3) *cheY*/YFP–CheY; (4) *cheZ*/CheZ–YFP; and (5) *cheZ*/YFP–CheZ.
B. Swarm ring formation by (1) RP437/pBAD18K wild type; (2) *fliM*/FliM–YFP; (3) *fliM*/YFP–FliM; (4) *cheA*/YFP–$CheA_L$; and (5) *cheA*/YFP–$CheA_S$. Swarm plates were supplemented with kanamycin (50 $\mu g\ ml^{-1}$).

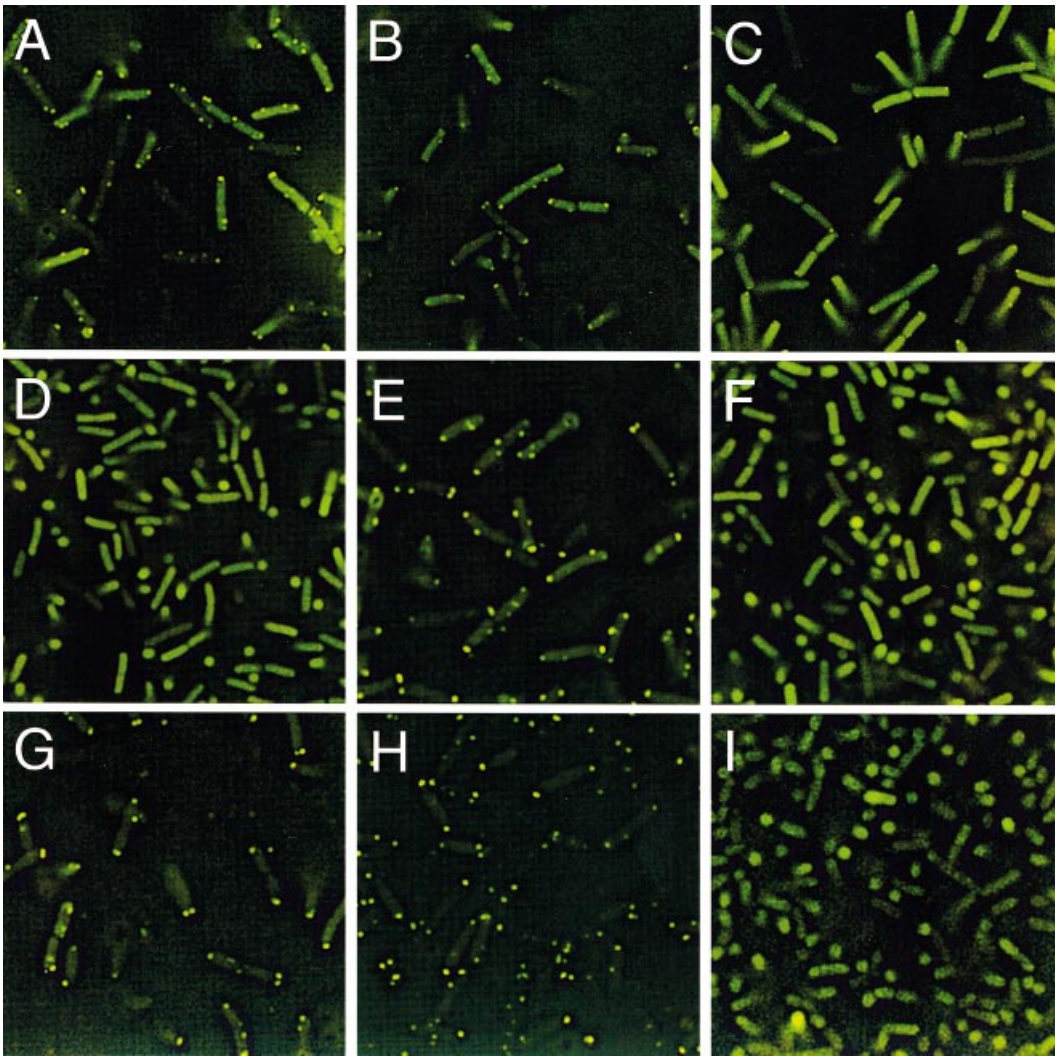

Fig. 2. Localization of YFP fusions to chemotaxis proteins in different mutant backgrounds.
A. CheY–YFP/*cheY*.
B. CheY–YFP/*trg*.
C. CheY–YFP/*tsr*.
D. CheY–YFP/*cheA*.
E. CheZ–YFP/*cheZ*.
F. CheZ–YFP/*cheA*.
G. YFP–$CheA_L$/*cheA*.
H. YFP–$CheA_S$/*cheA*.
I. YFP–$CheA_S$/*tar tsr tap trg*.
The arabinose concentration was 0.005%. Results for a larger set of mutant backgrounds are given in Table 2.

that gave an optimal (or nearly optimal) complementation, 0.002% arabinose for FliM–YFP and 0.005% arabinose for all the other proteins, was used for further experiments. Under these conditions, the levels of expression of the fusion proteins were close to the levels of expression of the native proteins (≈70–180%), and the total amount of degraded protein was small, always less than 10% of the amount of native protein (see *Experimental procedures*). Thus, it seems unlikely that degradation products could account for any of the observed complementation effects.

Association of YFP fusions with MCP clusters

Both CheY–YFP and YFP–CheY showed a similar pattern of localization. Two types of clusters were observed, intense polar clusters and weaker lateral clusters. Usually, in cells grown to late exponential phase, either one or two clusters were seen at the poles and none or one along the sides of a cell (Fig. 2A). This strongly resembles the clustering of MCPs observed previously by immunoelectron and immunofluorescent microscopy (Maddock and Shapiro, 1993).

Table 2. Localization of YFP fusions.

Fusion protein	Background														
	Wild type	*cheY*	*cheZ*	*tar*	*tsr*	*trg*	*tar tsr tap trg*	*cheW*	*cheA*	*cheA H48Q*	*fliM flgM*	*fliM*	*fliM fliG*	*fliM fliN*	*flhC*
CheY–YFP	1.40	1.61	1.42	1.19	1.18	1.31	NL	NL	NL	1.45	1.59	NL	ND	ND	NL
YFP–CheY	1.50	1.57	1.49	1.25	1.19	1.36	NL	NL	NL	1.45	1.60	NL	ND	ND	NL
CheZ–YFP	1.45	1.40	1.90	1.23	1.19	1.44	NL	NL	NL	ND	ND	ND	ND	ND	NL
YFP–CheZ	1.57	1.49	1.83	1.30	1.31	1.55	NL	NL	NL	ND	ND	ND	ND	ND	NL
YFP–$CheA_L$	1.50	ND	ND	1.32	1.31	1.50	NL	NL	1.88	ND	ND	ND	ND	ND	NL
YFP–$CheA_S$	1.74	ND	ND	1.46	1.52	1.69	NL	NL	2.24	ND	ND	ND	ND	ND	NL
FliM–YFP	1.48	ND	ND	ND	ND	ND	ND	ND	ND	ND	ND	1.58	NI	1.30	NI
YFP–FliM	1.42	ND	ND	ND	ND	ND	ND	ND	ND	ND	ND	1.55	NI	1.32	NI

The degree of localization was measured as the ratio of the integrated intensity of fluorescence of the localized protein to the integrated intensity of fluorescence of a region of the same size elsewhere in the same cell. More than 40 cells were measured for each fusion construct/strain combination. The standard errors of the measurements were ≤ 0.05. NL, non-localized; NI, non-localized with inclusion bodies in some cells; ND, not determined. See text for further comments.

To verify that CheY–YFP localizes with the MCPs, we analysed the distribution and intensity of CheY–YFP clusters in different *mcp*, *che* and *fli* backgrounds (Table 2; Fig. 2A–D). CheY–YFP clusters were seen in the wild type, *cheY*, *cheZ*, *tar*, *tsr* and *trg* backgrounds, but not in a mutant defective in *cheA*, a mutant defective in *cheW* or a mutant defective in all four MCPs (*tar tsr tap trg*). This is consistent with CheY localization on MCP clusters, mediated by CheW and CheA. In *tar* and *tsr* strains, which lack either one or other of the major MCP proteins, the intensity of CheY localization at the poles was significantly reduced, and lateral clusters nearly disappeared (Table 2; Fig. 2C). In a *trg* strain lacking a minor MCP protein, CheY localization was similar to that in the wild type (Table 2; Fig. 2B). Phosphorylation of CheY–YFP by CheA was not required for localization, as shown by the presence of clusters in the *cheAH48Q* mutant (Table 2). There was no CheY–YFP localization in *fliM* or *cheY fliM* mutants, but further investigation showed that this was a result of the negative effect of the *fliM* deletion on the expression of chemotaxis and receptor genes (Kutsukake and Iino, 1994). In the *fliM flgM* background, where the gene for the anti-sigma factor FlgM responsible for the negative control was deleted, normal localization of CheY–YFP was restored (Table 2).

To determine further whether we might see the localization of CheY–YFP on flagellar motors, we phosphorylated CheY–YFP *in vivo* under conditions that do not allow clustering of MCPs. First, we used acetate, which is known to cause CheA-independent CheY phosphorylation through the formation of acetyl phosphate (Wolfe *et al*., 1988; Lukat *et al*., 1992). The addition of acetate to the *cheY cheA* strain expressing CheY–YFP yielded no CheY–YFP localization (data not shown), although the cells became tumbly compared with the control, suggesting that the CheY–YFP fusion was phosphorylated and could bind to the motor. We also co-expressed CheY–YFP with a constitutively active cytoplasmic fragment of the Tsr receptor (Ames and Parkinson, 1994) in a *cheY tar tsr tap trg* strain. Again, the cells tumbled, but no CheY–YFP localization was seen on the motor (data not shown).

Two other chemotaxis proteins, CheZ and CheA, were expected to localize with the MCPs. Co-localization of CheZ–GFP and MCP was shown previously in the laboratory of Mike Manson (personal communication). We observed such localization for both YFP–CheZ and CheZ–YFP (Table 2; Fig. 2E). This localization was dependent on the presence of MCP, CheW and CheA, but not on the presence of CheY (Table 2; Fig. 2F). Both YFP–$CheA_L$ and YFP–$CheA_S$ localized in a pattern identical to that of CheY–YFP. This localization was dependent on the presence of MCP and CheW (Table 2; Fig. 2G-H). As the plasmid expressing YFP–$CheA_L$ also expresses unlabelled $CheA_S$, one might expect less fluorescence in the clusters for YFP–$CheA_L$ because of competition between the two. This appears to be the case, as indicated in Table 2.

To verify the co-localization of the CheY, CheZ and CheA fusion proteins with MCP clusters, we performed additional staining using primary antibody raised against the signalling domain of Tsr, in combination with Texas red-coupled secondary antibody (Fig. 3). Cell fixation with methanol and treatment with lysozyme, necessary to make *E. coli* cells permeable to antibodies, led to some loss of CheY–YFP, as evidenced by a reduction in the overall level of green fluorescence. At the same time, some cells were not permeabilized enough to allow MCP staining. However, in most cells, presumably cells that were partially lysed, the remaining CheY–YFP spots co-localized precisely with the MCP clusters (Fig. 3A–C). We tried other fixatives, e.g. paraformaldehyde, formaldehyde and glutaraldehyde, but CheY–YFP localization was lost. However, there was no loss of the other fusion proteins,

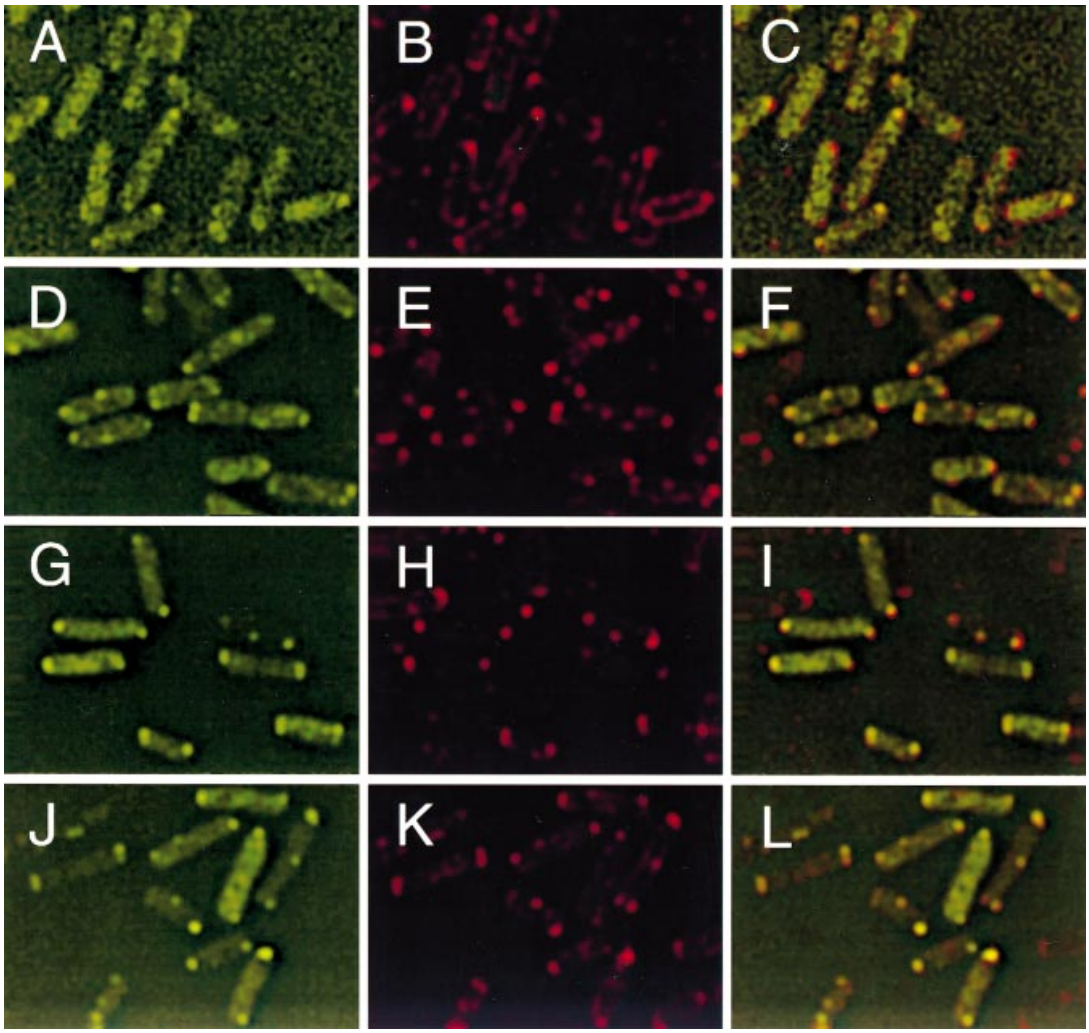

Fig. 3. Association of CheY, CheZ and CheA fusion proteins with MCP clusters, demonstrated by immunofluorescence. Cells expressing YFP fusions were fixed with methanol, stained with anti-Tsr antibody and counterstained with anti-rabbit Texas red-coupled antibody, as described in *Experimental procedures*.
A–C. *cheY* cells expressing CheY–YFP.
D–F. *cheZ* cells expressing CheZ–YFP.
G–I. *cheA* cells expressing YFP–$CheA_L$.
J–L. *cheA* cells expressing YFP–$CheA_S$.
Left: YFP fluorescence (green); centre: Texas red fluorescence (red); right: superimposition of the images from the left and centre. Orange colour shows co-localization of CheY (C), CheZ (F), $CheA_L$ (I) and $CheA_S$ (L) fusion proteins with MCP clusters.

which remained associated with the MCP clusters (Fig. 3D–K).

Results obtained by immunoelectron microscopy suggest that, although CheW and CheA are important for MCP clustering (Maddock and Shapiro, 1993), there is a significant level of clustering in the absence of CheA (Skidmore *et al*., 2000). To learn whether the mere delocalization of MCPs could account for the absence of localization of the chemotaxis fusion proteins in the *cheW* and *cheA* backgrounds, we compared MCP localization in wild-type, *cheA* and *cheW* strains (Fig. 4A–C). In the absence of CheA or CheW, MCPs were still localized to the poles (Fig. 4B and C), although not in tight clusters (Fig. 4A). Thus, it is the missing interaction with CheA (for CheY and CheZ) and with CheW (for CheA) that prevents the fusion proteins from being localized to the poles.

FliM–YFP localization on flagellar motors

In addition to the localization of chemotaxis proteins on MCP clusters, we also observed the localization of FliM on flagellar motors. Although FliM–YFP was much more efficient than YFP–FliM in complementing a *fliM* mutant for spreading in soft agar (Fig. 1B, swarms 2 and 3), both

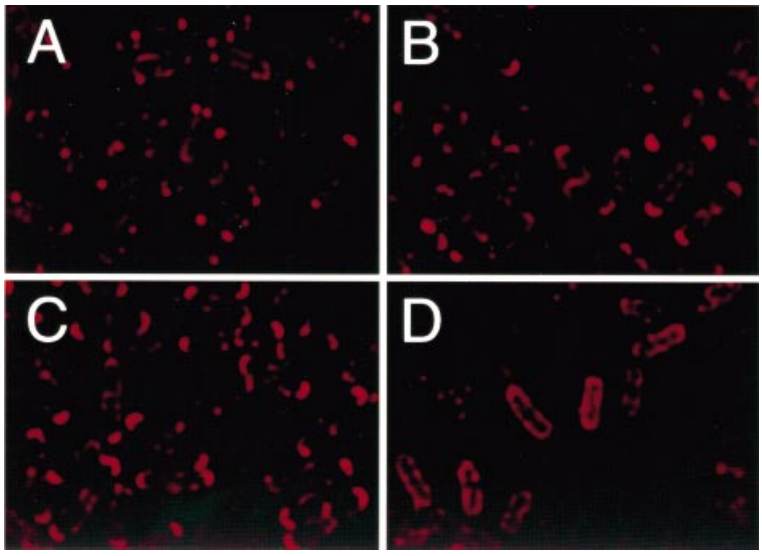

Fig. 4. Localization of MCPs in different mutant backgrounds, demonstrated by immunofluorescence. Wild type (A), *cheA* (B), *cheW* (C) and *tar tsr tap trg* (D) cells were fixed and stained with anti-Tsr antibody, as described in the legend to Fig. 3. In wild-type cells, MCPs are tightly clustered (A). In the *cheA* or *cheW* background, they remain localized at the cell poles, but more diffusely (B and C). This localization is not observed in the *mcp* strain.

constructs complemented the cells for flagellation and motility and showed the same pattern of localization (Table 2; Fig. 5A). This pattern showed several spots (up to 10), more or less evenly distributed along the cell body. As FliM is known to be a part of the cytoplasmic C-ring of the flagellar motor, these spots probably correspond to motors distributed at random on the surface of the cell. In some cells, a bright fluorescent spot was also observed at the end of the cell, presumably corresponding to an inclusion body. The localization of FliM–YFP was dependent on another constituent of the cytoplasmic C-ring, FliG (Fig. 5C), which is known to be assembled on the C-ring before FliM (Zhao *et al*., 1995). The absence of yet another C-ring component, FliN, did not abolish FliM–YFP localization (Fig. 5B), in agreement with the observation that FliM binds to FliG in the absence of FliN (Marykwas *et al*., 1996; Tang *et al*., 1996). The formation of a single protein aggregate (inclusion body) by FliM–YFP in some *fliM* cells, in many *fliM fliG* cells or in a *flhC* strain suggests that proper targeting to the motor reduces the free concentration of FliM and, hence, the likelihood that it forms inclusion bodies. This is consistent with the finding that, under normal growth conditions, wild-type FliM tends to form aggregates of high molecular weight (Zhao *et al*., 1996).

The localization of FliM–YFP to flagellar motors was confirmed by immunofluorescence. We used a primary antibody against flagellar hooks and a secondary antibody coupled with Texas red. These experiments were carried out in a *fliC* strain that lacks flagellar filaments but has hooks (Fig. 6). An additional mutation, *clpP*, which inactivates a component of one of the major *E. coli* proteases, was introduced in the *fliM fliC* background strain (GP90). This reduces the level of FliM–YFP

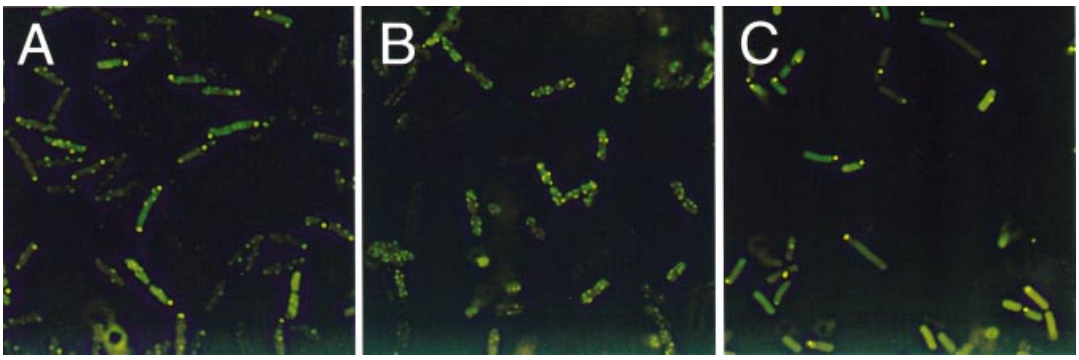

Fig. 5. Localization of FliM–YFP in different mutant backgrounds.
A. *fliM*.
B. *fliM fliN*.
C. *fliM fliG*.
The arabinose concentration was 0.002%.

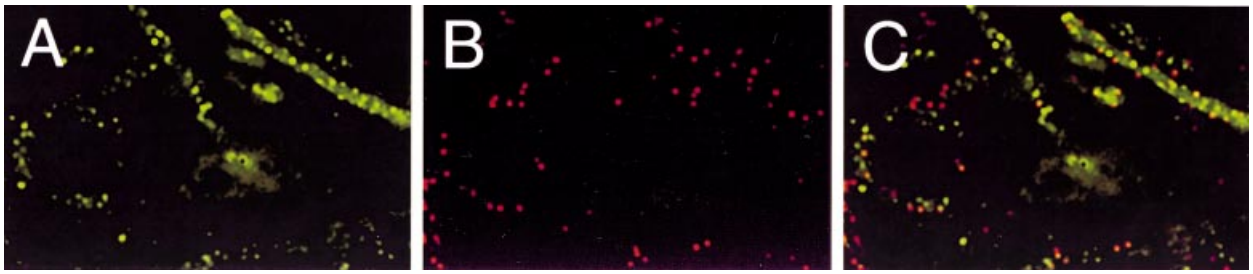

Fig. 6. Association of FliM–YFP with flagellar motors, demonstrated by immunofluorescence. *fliM fliC* cells expressing FliM–YFP were stained with antihook antibody and counterstained with anti-rabbit Texas red-coupled antibody, as described in *Experimental procedures*.
A. FliM–YFP (green).
B. Flagellar hooks (red).
C. Superimposition of the images in (A) and (B). All the red spots (hooks) are close to or overlap with the green spots (FliM–YFP). Additional green spots represent immature motors (motors with C-rings but without hooks).

degradation to $<2\%$ without interfering with FliM–YFP function. As shown in Fig. 6C, green FliM–YFP spots (Fig. 6A) co-localized with red hook spots (Fig. 6B). However, not all of the green FliM–YFP spots had a corresponding red hook spot. This is expected, as many motors that have yet to synthesize hooks contain FliM (Aizawa, 1996). However, the brightest FliM–YFP foci were not associated with the hooks. Currently, we do not have an explanation for this fact. We do not know why incomplete motors should be brighter. And it seems unlikely that the brighter spots are inclusion bodies, because there is generally only one inclusion body formed per cell in the *fliG* background (Fig. 5C), even when the cells are made filamentous by growth in the presence of cephalexin (data not shown).

Discussion

Two protein complexes are of particular importance in bacterial chemotaxis: the receptor complex, consisting of MCPs and associated proteins; and the switch complex, assembled on the cytoplasmic face of the flagellar motor. The clustering of receptor complexes adds an additional level of complexity and could be important for signal amplification (Bray *et al*., 1998; Levit *et al*., 1998; Duke and Bray, 1999). We used YFP fusions to study the localization of a number of the components of these complexes. Except for CheA, the fusions were functional and restored chemotaxis in the corresponding null mutant background. The present results (together with the work of M. Manson, in preparation) provide direct visualization of receptor and switch complexes in living cells.

Our data imply the existence of a stable complex in which CheW, CheA, CheY and CheZ co-localize with MCP. We did not make a CheW fusion, but CheW was required for association of the other components, in agreement with previous studies (Ninfa *et al*., 1991; Gegner *et al*., 1992; Maddock and Shapiro, 1993). The deletion of either of the genes that encodes a major MCP, *tar* or *tsr*, decreases the degree of localization of CheA, CheY or CheZ, but it does not abolish it. This is consistent with the suggestion that different MCP proteins are intermixed in the same clusters (Stock and Levit, 2000). None of the fusion proteins formed clusters in strains that were deleted for all of the MCPs or for CheW; therefore, their localization is not an artifact resulting from the formation of inclusion bodies. CheW is required for localization of CheA, and CheA is required for localization of both CheY and CheZ; however, CheY and CheZ localize independently. As MCPs localize at the poles in the absence of CheW or CheA, the localization of CheY and CheZ must result from their binding to the MCP–CheW–CheA ternary complex, not to MCP directly.

We were also able to observe assembly of FliM–YFP on the switch complex. If a motor had a hook, as indicated by immunofluorescence, it also had a switch complex, as indicated by fluorescence of FliM–YFP. However, not all motors had hooks. FliM localization was not observed in a *flhC* strain, where flagellar synthesis does not occur. Nor was it observed in the absence of FliG, in support of a mediatory role for FliG in FliM attachment. FliN was not required for the FliM localization as long as FliG was present, consistent with the biochemical evidence for FliM, FliG binding (Marykwas and Berg, 1996; Marykwas *et al*., 1996; Tang *et al*., 1996). A possible explanation for the absence of FliM in basal body preparations from *fliN* mutants (Zhao *et al*., 1995) is that FliN stabilizes the attachment of FliM to FliG, which is otherwise lost in the purification procedure. We did observe somewhat lower intensity of FliM localization in a *fliN* background.

However, we were not able to observe localization of CheY fusion proteins to the switch complex, even under conditions in which cells tumbled. This might be a signal-to-background problem, as there are many more CheY molecules in the cell than there are FliM binding sites. On the other hand, there are a relatively large number of components with which to build CheW–CheA–MCP

complexes and a relatively small number of molecules of FliM (see Bray *et al*., 1993).

An obvious advantage in the use of YFP (or other GFP) fusions is that the architecture of receptor and motor complexes can be probed in living cells. Our results complement those obtained by immunofluorescence and protein purification.

Experimental procedures

Strains and plasmids

E. coli strains used in this work were derived from strain RP437, a K-12 derivative that is wild type for chemotaxis (Parkinson and Houts, 1982). All strains and plasmids are listed in Table 3. LB (Luria–Bertani) medium or tryptone broth (TB; 1% tryptone, 0.5% NaCl) was used for *E. coli* cultures. Ampicillin was used at 100 μg ml^{-1} and kanamycin at 50 μg ml^{-1}. Chemotaxis tests were performed on TB soft agar plates (1% tryptone, 0.5% NaCl, 0.3% Difco agar).

DNA methods

E. coli plasmid DNA was purified using the QIAprep Spin Miniprep Kit (Qiagen). Polymerase chain reaction (PCR) was performed in a MiniCycler (MJResearch) using *Pwo* DNA polymerase (Boehringer Mannheim). PCR primers used in this study are listed in Table 4; they were from Integrated DNA Technologies. Sequencing was carried out at the Harvard MCB sequencing facility.

Strain construction

An in frame deletion in *cheY* (codons 8–122) was generated *in vitro* using two PCR steps, as described by Higuchi (1989), with pRL22 as template and the primers listed in Table 4.

Table 3. Bacterial strains and plasmids used in this study.

Strain or plasmid	Relevant genotype/phenotype	Reference or source
Strains		
RP437	Wild type for chemotaxis	Parkinson and Houts (1982)
RP9535	Δ*cheA*	J. S. Parkinson
RP1616	Δ*cheZ*	J. S. Parkinson
RP3021	*cheW*	J. S. Parkinson
RP4532	Δ*tar*	J. S. Parkinson
RP5714	Δ*tsr*	J. S. Parkinson
RP1131	*trg::*Tn*10*	J. S. Parkinson
RP3098	Δ*(flhC–flhA)*	J. S. Parkinson
HCB339	Δ*(tar–tap)* Δ*tsr trg::*Tn*10*	J. S. Parkinson
DFB190	*fliM* null strain, *fliM::cam*	Tang and Blair (1995)
DFB228	*fliM* null strain, in frame *fliM* deletion	D. F. Blair
DFB232	*fliM fliN* null strain	D. F. Blair
DFB247	*fliM fliG* null strain	D. F. Blair
GP90	*fliM::cam fliC::*Tn*10 clpP::cam recA::kan*	P. Danese
VS100	Δ*cheY*, in frame *cheY* deletion	This work
VS103	Δ*cheY fliM::cam* Δ*flgM*	This work
Plasmids		
pBAD18K	Expression vector, P_{BAD} promoter, Km^R; parent of pVS1, pVS5, pVS11, pVS30, pVS50, pVS53, pVS56, pVS59	Guzman *et al.* (1995)
pBAD30	Expression vector, P_{BAD} promoter, Ap^R; parent of pVS13	Guzman *et al.* (1995)
pBAD33	Expression vector, P_{BAD} promoter, Cm^R, pACYC ori; parent of pVS15, pVS17	Guzman *et al.* (1995)
pEYFP	YFP expression plasmid, Ap^R	Clontech
pRL22	CheY expression plasmid, Ap^R	Matsumura *et al.* (1984)
pDFB72	FliM expression plasmid, Ap^R	Tang and Blair (1995)
pDV4	CheA expression plasmid, Ap^R	Hess *et al.* (1987)
pDV4cheA48HQ	CheA48HQ expression plasmid, Ap^R	Oosawa *et al.* (1988)
pVS1	CheY–YFP expression plasmid, Km^R	This work
pVS5	YFP–CheY expression plasmid, Km^R	This work
pVS11	FliM–YFP expression plasmid, Km^R	This work
pVS13	FliM–YFP expression plasmid, Ap^R	This work
pVS15	CheY–YFP expression plasmid, Cm^R	This work
pVS17	YFP–CheY expression plasmid, Cm^R	This work
pVS30	YFP–FliM expression plasmid, Km^R	This work
pVS50	YFP–CheZ expression plasmid, Km^R	This work
pVS53	CheZ–YFP expression plasmid, Km^R	This work
pVS56	YFP–$CheA_L$ expression plasmid, Km^R	This work
pVS59	YFP–$CheA_s$ expression plasmid, Km^R	This work
pPA56	$Tsr_{290-470}$ expression plasmid, Ap^R	Ames and Parkinson (1994)
pAMPTS	Cloning vector, ts origin of replication, Ap^R; parent of pVS20, pVS21	G. J. Phillips, personal gift
pVS20	Δ*cheY* construct, Ap^R	This work
pVS21	Δ*flgM* construct, Ap^R	This work

Table 4. Primers used in this study.

Primer	Sequence[a]	Priming site[b]
Fusions		
CheY–EYFP		
PCHEY	5-′CCGGACAGGAGCTCCGTATTTAAATC-3′	−37→−11 (*cheY*)
VIC1	5′-GCTCACCA*CTCCTCCGCC*GCCCAGTTTCTCAAAGAT-3′	384→366 (*cheY*compl)[c]
VIC2	5′-*GGCGGAGGA*GTGGTGAGCAAGGGCGAGGAG-3′	2→21 (*eyfp*)
VIC3	5′-TCAGTTGGAATTCTAGAGTC-3′	749→729 (*eyfp*compl)
EYFP–CheY		
VIC20	5′-TCGCCACCGAGCTCAGGAGTGTGAAATGGTGAGCAAGGGCGAGGAG-3′	1→20 (*eyfp*)
VIC11	5′-*TCCGCCTCCGCCTCC*CTTGTACAGCTCGTCCATG-3′	716→698 (*eyfp*compl)
VIC10	5′-*GGAGGCGGAGGCGGA*GTGGCGGATAAAGAAC-3′	2→17 (*cheY*)
VIC18	5′-GTCAGCAGGTCTAGATTGATGGTTGC-3′	429→405 (*cheY*compl)
FliM–EYFP		
VIC12	5′-GCTGTAGAGCTCTTTTATTCTGCGATAACGAC-3′	−20→0 (*fliM*)
VIC9	5′-*TCCGCCTCCGCCTCC*TTTGGGCTGTTCCTCGTT-3′	1001→948 (*fliM*compl)
VIC21	5′-*GGAGGCGGAGGCGGA*GTGGTGAGCAAGGGCGAGGAG-3′	2→21 (*eyfp*)
VIC3	(See above)	
EYFP–FliM		
VIC20	(See above)	
VIC11	(See above)	
VIC54	5′-*GGAGGCGGAGGCGGA*GTGGGCGATAGTATTCTTTCTCAAGCTG-3′	2→27 (*fliM*)
VIC55	5′-CCGGATTCTAGATGTCACTCATTTGGGCTG-3′	1022→993 (*fliM*compl)
CheZ–EYFP		
VIC61	5′-ATGTTTGAGCTCCAGGGCATGTGAGG-3′	−33→−8 (*cheZ*)
VIC60	5′-*TCCGCCTCCGCCTCC*AAATCCAAGACTATCCAAC-3′	641→623 (*cheZ*compl)
VIC21	(See above)	
VIC3	(See above)	
EYFP–CheZ		
VIC20	(See above)	
VIC11	(See above)	
VIC58	5′-*GGAGGCGGAGGCGGA*CAACCATCAATCAAACCTGC-3′	7→25 (*cheZ*)
VIC59	5′-TCGCCTTCTAGACCGCCTGATATG-3′	699→675 (*cheZ*compl)
EYFP–CheA$_L$		
VIC20	(See above)	
VIC11	(See above)	
VIC62	5′-*GGAGGCGGAGGCGGA*GATATAAGCGATTTTTATCAG-3′	10→30 (*cheA*)
VIC63	5′-GTTACATTCTAGATACCGGTCATATTG-3′	2007→1981 (*cheA*compl)
EYFP–CheA$_S$		
VIC20	(See above)	
VIC11	(See above)	
VIC64	5′-*GGAGGCGGAGGCGGA*GTGCAAGAACAGCTCGACGC-3′	292–310 (*cheA*)
VIC63	(See above)	
cheY deletion		
VIC14	5′-ATCGGCCTTCTAGATGTGTTGTTCCATTC-3′	−298→−268 (*cheY*)
VIC15	5′-TCCTCACATGCCCAGTTTAAGTTCTTTATCCGCC-3′	20→2 (*cheY*compl)
VIC16	5′-CTGGGCATGTGAGGATGCG-3′	378→396 (*cheY*)
VIC19	5′-ATCTGGCAGAATTCTCGTGTATCTG-3′	759→734 (*cheY*compl)

a. Introduced restriction sites (*Sac*I, *Xba*I or *Eco*RI) are underlined; sequences encoding glycine linkers are marked in italics.
b. Relative to the transcriptional start site (+1) of the corresponding gene.
c. Complementary strand.

Outer primers were designed to contain *Eco*RI (VIC19) and *Xba*I (VIC14) restriction sites, and these sites were used to clone the fragment into the temperature-sensitive pAMPTS vector. The resulting construct, pVS20, was transformed in *E. coli* and grown on LB plates with ampicillin at 30°C. Transformants were streaked on LB–ampicillin plates and grown overnight at 42°C, allowing only the growth of cells that integrated the pVS20 construct into the chromosome. From these plates, single colonies were picked, grown for 24 h in LB at 30°C without selection, plated at serial dilutions on LB–ampicillin plates and grown overnight at 30°C. The colonies were then tested for ampicillin resistance and chemotaxis on soft agar plates.

Construction of YFP fusion proteins

YFP fusions to chemotaxis proteins and FliM were constructed using PCR. The target gene and the *eyfp* gene (Clontech) were amplified using primers with complementary overhangs, encoding either a 3× or a 5× glycine linker (Table 4). The resulting DNA fragments were annealed and amplified in a second round of PCR to form a fragment encoding a fusion protein with either a 3× Gly or a 5× Gly linker between the target protein and YFP. Outer primers were designed to contain *Sac*I and *Xba*I restriction sites, and these were used to clone fragments into the arabinose-inducible pBAD18K expression vector. The final constructs

were sequenced to ensure no PCR mistakes. Expression of full-length fusion proteins was verified by immunoblot using antibodies against FliM, CheY, CheZ and/or YFP (see below). Immunoblots were quantified using the program NIH IMAGE. The levels of expression of fusion proteins (compared with native proteins) estimated from immunoblots were as follows: CheY–YFP, ≈90%; YFP–CheY, ≈70%; CheZ–YFP, ≈110%; YFP–CheZ, ≈70%; YFP–$CheA_L$, ≈120%; YFP–$CheA_S$, ≈180%; FliM–YFP, ≈150%; YFP–FliM, ≈100%. The total levels of degradation products were: CheY–YFP and YFP–CheY, <3%; FliM–YFP and YFP–FliM, <10%; CheZ–YFP, <10%; YFP–CheZ, not detected; YFP–$CheA_L$ and YFP–$CheA_S$, not detected. FliM–YFP degradation was further reduced to <2% by the introduction of a *clpP* mutation (ClpP is a component of the ClpAP protease) in the background strain (GP90) without loss of motor function. Functionality of fusion proteins was tested by the restoration of chemotaxis on soft agar plates supplemented with kanamycin (50 μg ml^{-1}) and arabinose (0.001–0.005%).

Immunoblots

Immunoblots were performed as described previously with minor modifications (Scharf *et al*., 1998). Motile cells expressing fusion proteins were grown as described below. Whole-cell extracts were prepared from 10 ml samples. Cells were washed once with PBS, resuspended in 300 μl of PBS and lysed by sonication. SDS–PAGE loading buffer (3×) was added, samples were boiled at 95°C for 5 min, and 5 μl of each sample was loaded onto an SDS gradient (8–15%) polyacrylamide gel. After separation by electrophoresis, the proteins were electroblotted to a Hybond ECL nitrocellulose membrane using a tank blot device (Bio Labs, Harvard University) for 3 h at 60 V in transfer buffer (25 mM Tris, 192 mM glycine, 0.05% SDS, 20% methanol, pH 8.3). Blots were blocked overnight at room temperature in TBS-T [20 mM Tris-HCl, 140 mM NaCl, 0.1% (v/v) Tween 20, pH 7.6] with 5% blocking reagent (instant non-fat dry milk) on a rocking platform. Blots were then incubated with primary antibodies in TBS-T for 2 h at room temperature. Monoclonal anti-GFP antibodies (Clontech) were used at a 1:1500 dilution, monoclonal anti-CheY and anti-CheZ antibodies (Scharf *et al*., 1998) at a 1:1000 dilution and polyclonal anti-FliM antibodies (a gift from David Blair) at a 1:1000 dilution. Blots were washed three times (15 min each) with TBS-T, incubated for 2 h with sheep anti-mouse (or anti-rabbit) horseradish peroxidase-linked secondary antibodies (Amersham) diluted 1:2500 in TBS-T, washed again and detected using an ECL kit (Amersham), as described by the manufacturer.

Growth conditions and fluorescence microscopy

Motile cell cultures were grown in tryptone broth (TB) with kanamycin (50 μg ml^{-1}) at 33°C. To obtain motile cells expressing YFP fusions for fluorescence measurements, overnight cultures were diluted 1:100 in TB containing arabinose (0.002–0.005%, as indicated in the text) and allowed to grow for 4 h in a rotary shaker. A cell suspension (100 μl) was applied to a polylysine-coated coverslip, incubated for 5 min and washed three times with tethering buffer (Block *et al*., 1983) before microscopy.

For double staining with FliM–YFP and polyclonal antihook antibody (Ishihara *et al*., 1983), cells from a 1 ml culture were resuspended in 100 μl of tethering buffer and incubated with antibody at a 1:500 dilution for 20 min. Cells were washed three times with tethering buffer and incubated in 100 μl of tethering buffer with secondary goat anti-rabbit Texas red-conjugated antibodies (1:300 dilution; Molecular Probes) for another 20 min. After incubation, cells were washed with tethering buffer, applied to a polylysine-coated coverslip, washed with tethering buffer once more and imaged.

For double staining with CheY–YFP and anti-Tsr antibody, cells from a 1 ml culture were fixed using methanol as described previously (Teleman *et al*., 1998). Fixed cells were placed on a polylysine-coated coverslip, allowed to dry fully and treated with lysozyme (2 mg ml^{-1}) in GTE buffer (50 mM glucose, 25 mM Tris, 1 mM EDTA, pH 7.5) for 10 min. Coverslips were incubated with a blocking solution (2% BSA in PBS, pH 7.5) overnight at 4°C, incubated in 2% BSA–PBS with anti-Tsr antibodies (1:500 dilution; a gift from Sandy Parkinson) for 2 h at room temperature, washed 10 times with PBS, incubated with secondary goat anti-rabbit Texas red antibody (1:300 dilution in 2% BSA–PBS) for 2 h at room temperature, washed with PBS again and imaged.

Fluorescent microscopy was performed using a Delta Vision deconvolution microscope and program package (Applied Precision). YFP images were taken using a bandpass excitation filter (480–500 nm) and either a long-pass emission filter (510 nm) or, if cells were also stained with Texas red, a bandpass emission filter (509–547 nm). Texas red images were taken using a bandpass excitation filter (541–569 nm) and a bandpass emission filter (581–654 nm). When necessary, images were quantified using the program NIH IMAGE. Deconvoluted images were prepared for final publication using Adobe Photoshop 5.5 and a Tektronix Phaser 450 printer.

Acknowledgements

We thank Paul Danese for inspiration and help during the early phases of this study. This work was supported by grant AI16478 from the National Institute of Allergy and Infectious Diseases and by the Rowland Institute for Science.

References

Aizawa, S.-I. (1996) Flagellar assembly in *Salmonella typhimurium*. *Mol Microbiol* **19**: 1–5.

Alon, U., Camarena, L., Surette, M.G., Aguera y Arcas, B., Liu, Y., Leibler, S., *et al*. (1998) Response regulator output in bacterial chemotaxis. *EMBO J* **17**: 4238–4248.

Ames, P., and Parkinson, J.S. (1994) Constitutively signalling fragments of Tsr, the *Escherichia coli* serine chemoreceptor. *J Bacteriol* **176**: 6340–6348.

Bilwes, A.M., Alex, L.A., Crane, B.R., and Simon, M.I. (1999) Structure of CheA, a signal-transducing histidine kinase. *Cell* **96**: 131–141.

Block, S.M., Segall, J.E., and Berg, H.C. (1983) Adaptation kinetics in bacterial chemotaxis. *J Bacteriol* **154**: 312–323.

Borkovich, K.A., Kaplan, N., Hess, J.F., and Simon, M.I. (1989) Transmembrane signal transduction in bacterial chemotaxis involves ligand-dependent activation of phosphate group transfer. *Proc Natl Acad Sci USA* **86**: 1208–1212.

Bray, D., Bourret, R.B., and Simon, M.I. (1993) Computer simulation of the phosphorylation cascade controlling bacterial chemotaxis. *Mol Biol Cell* **4**: 469–482.

Bray, D., Levin, M.D., and Morton-Firth, C.J. (1998) Receptor clustering as a cellular mechanism to control sensitivity. *Nature* **393**: 85–88.

Conn, P.M. (ed.) (1999) Green fluorescent protein. *Methods Enzymol* **302**.

Djordjevic, S., and Stock, A.M. (1998) Structural analysis of bacterial chemotaxis proteins: components of a dynamic signaling system. *J Struct Biol* **124**: 189–200.

Duke, T.A.J., and Bray, D. (1999) Heightened sensitivity of a lattice of membrane receptors. *Proc Natl Acad Sci USA* **96**: 10104–10108.

Falke, J.J., Bass, R.B., Butler, S.L., Chervitz, S.A., and Danielson, M.A. (1997) The two-component signaling pathway of bacterial chemotaxis: a molecular view of signal transduction by receptors, kinases, and adaptation enzymes. *Annu Rev Cell Dev Biol* **13**: 457–512.

Francis, N.R., Sosinsky, G.E., Thomas, D., and DeRosier, D.J. (1994) Isolation, characterization and structure of bacterial flagellar motors containing the switch complex. *J Mol Biol* **235**: 1261–1270.

Gegner, J.A., Graham, D.R., Roth, A.F., and Dahlquist, F.W. (1992) Assembly of an MCP receptor, CheW, and kinase CheA complex in the bacterial chemotaxis signal transduction pathway. *Cell* **18**: 975–982.

Guzman, L.-M., Belin, D., Carson, M.J., and Beckwith, J. (1995) Tight regulation, modulation, and high-level expression by vectors containing the arabinose P_{BAD} promoter. *J Bacteriol* **177**: 4121–4130.

Hess, F., Oosawa, K., Matsumura, P., and Simon, M.I. (1987) Protein phosphorylation is involved in bacterial chemotaxis. *Proc Natl Acad Sci USA* **84**: 7609–7613.

Hess, F., Oosawa, K., Kaplan, N., and Simon, M.I. (1988a) Phosphorylation of three proteins in the signaling pathway of bacterial chemotaxis. *Cell* **53**: 79–87.

Hess, J.F., Bourret, R.B., and Simon, M.I. (1988b) Histidine phosphorylation and phosphoryl group transfer in bacterial chemotaxis. *Nature* **336**: 139–143.

Higuchi, R. (1989) Using PCR to engineer DNA. In *PCR Technology: Principles and Applications for DNA Amplification*. Erlich, H.A. (ed.). New York: Stockton, pp. 61–70.

Ishihara, A., Segall, J.E., Block, S.M., and Berg, H.C. (1983) Coordination of flagella on filamentous cells of *Escherichia coli*. *J Bacteriol* **155**: 228–237.

Khan, I.M., Reese, T.S., and Khan, S. (1992) The cytoplasmic component of the bacterial flagellar motor. *Proc Natl Acad Sci USA* **89**: 5956–5960.

Khan, S., Zhao, R., and Reese, T.S. (1998) Architectural features of the *Salmonella typhimurium* flagellar motor switch revealed by disrupted C-rings. *J Struct Biol* **122**: 311–319.

Kim, K.K., Yokota, H., and Kim, S.-H. (1999) Four-helical-bundle structure of the cytoplasmic domain of a serine chemotaxis receptor. *Nature* **400**: 787–792.

Kofoid, E.C., and Parkinson, J.S. (1991) Tandem translation starts in the cheA locus of *Escherichia coli*. *J Bacteriol* **173**: 2116–2119.

Kubori, T., Yamaguchi, S., and Aizawa, S.-I. (1997) Assembly of the switch complex onto the MS ring complex of *Salmonella typhimurium* does not require any other flagellar proteins. *J Bacteriol* **179**: 813–817.

Kuo, S.C., and Koshland, D.E. (1989) Multiple kinetic states for the flagellar motor switch. *J Bacteriol* **171**: 6279–6287.

Kutsukake, K., and Iino, T. (1994) Role of the FliA-FlgM regulatory system on the transcriptional control of the flagellar regulon and flagellar formation in *Salmonella typhimurium*. *J Bacteriol* **176**: 3598–3603.

Levit, M.N., Liu, Y., and Stock, J.B. (1998) Stimulus response coupling in bacterial chemotaxis: receptor dimers in signalling arrays. *Mol Microbiol* **30**: 459–466.

Liu, Y., Levit, M., Lurz, R., Surette, M.G., and Stock, J.B. (1997) Receptor-mediated protein kinase activation and the mechanism of transmembrane signaling in bacterial chemotaxis. *EMBO J* **16**: 7231–7240.

Lukat, G.S., McCleary, W.R., Stock, A.M., and Stock, J.B. (1992) Phosphorylation of bacterial response regulator proteins by low molecular weight phospho-donors. *Proc Natl Acad Sci USA* **89**: 718–722.

Lybarger, S.R., and Maddock, J.R. (1999) Clustering of the chemoreceptor complex in *Escherichia coli* is independent of the methyltransferase CheR and the methylesterase CheB. *J Bacteriol* **181**: 5527–5529.

Maddock, J.R., and Shapiro, L. (1993) Polar location of the chemoreceptor complex in the *Escherichia coli* cell. *Science* **259**: 1717–1723.

Margolin, W. (2000) Green fluorescent protein as a reporter for macromolecular localization in bacterial cells. *Methods* **20**: 62–72.

Marykwas, D.L., and Berg, H.C. (1996) A mutational analysis of the interaction between FliG and FliM, two components of the flagellar motor of *Escherichia coli*. *J Bacteriol* **178**: 1289–1294.

Marykwas, D.L., Schmidt, S.A., and Berg, H.C. (1996) Interacting components of the flagellar motor of *Escherichia coli* revealed by the two-hybrid system in yeast. *J Mol Biol* **256**: 564–576.

Matsumura, P., Rydel, J.J., Linzmeier, R., and Vacante, D. (1984) Overexpression and sequence of the *Escherichia coli cheY* gene and the biochemical activities of the CheY protein. *J Bacteriol* **160**: 36–41.

Ninfa, E.G., Stock, A., Mowbray, S., and Stock, J. (1991) Reconstitution of the bacterial chemotaxis signal transduction system from purified components. *J Biol Chem* **266**: 9764–9770.

Oosawa, K., Hess, J.F., and Simon, M.I. (1988) Mutants defective in bacterial chemotaxis show modified protein phosphorylation. *Cell* **53**: 89–96.

Oosawa, K., Ueno, T., and Aizawa, S.-I. (1994) Overproduction of the bacterial flagellar switch proteins and their interactions with the MS ring complex *in vitro*. *J Bacteriol* **155**: 265–274.

Parkinson, J.S., and Houts, S.E. (1982) Isolation and

behavior of *Escherichia coli* deletion mutants lacking chemotaxis functions. *J Bacteriol* **151**: 106–113.

Sanders, D.A., Gillece-Castro, B.L., Stock, A.M., Burlingame, A.L., and Koshland, D.E., Jr (1989) Identification of the site of phosphorylation of the chemotaxis response regulator protein, CheY. *J Biol Chem* **264**: 21770–21778.

Scharf, B.E., Fahrner, K.A., Turner, L., and Berg, H.C. (1998) Control of direction of flagellar rotation in bacterial chemotaxis. *Proc Natl Acad Sci USA* **95**: 201–206.

Schuster, S.C., Swanson, R.V., Alex, L.A., Bourret, R.B., and Simon, M.I. (1993) Assembly and function of a quaternary signal transduction complex monitored by surface plasmon resonance. *Nature* **365**: 343–347.

Skidmore, J.M., Ellefson, D.D., McNamara, B.P., Couto, M.M.P., Wolfe, A.J., and Maddock, J.R. (2000) Polar clustering of the chemoreceptor complex in *Escherichia coli* occurs in the absence of complete CheA function. *J Bacteriol* **182**: 967–973.

Stock, J., and Levit, M. (2000) Signal transduction: hair brains in bacterial chemotaxis. *Curr Biol* **10**: R11–R14.

Tang, H., and Blair, D.F. (1995) Regulated underexpression of the FliM protein of *Escherichia coli* and evidence for a location in the flagellar motor distinct from the MotA/MotB torque generators. *J Bacteriol* **177**: 3485–3495.

Tang, H., Braun, T.F., and Blair, D.F. (1996) Motility protein complexes in the bacterial flagellar motor. *J Mol Biol* **261**: 209–221.

Teleman, A.A., Graumann, P.L., Lin, D.C.-H., Grossman, A.D., and Losick, R. (1998) Chromosome arrangement within a bacterium. *Curr Biol* **8**: 1102–1109.

Wang, H., and Matsumura, P. (1996) Characterization of the $CheA_S$/CheZ complex: a specific interaction resulting in enhanced dephosphorylating activity on CheY-phosphate. *Mol Microbiol* **19**: 695–703.

Wang, H., and Matsumura, P. (1997) Phosphorylating and dephosphorylating protein complexes in bacterial chemotaxis. *J Bacteriol* **179**: 287–289.

Welch, M., Oosawa, K., Aizawa, S.-I., and Eisenbach, M. (1993) Phosphorylation-dependent binding of a signal molecule to the flagellar switch of bacteria. *Proc Natl Acad Sci USA* **90**: 8787–8791.

Wolfe, A.J., Conley, M.P., and Berg, H.C. (1988) Acetyladenylate plays a role in controlling the direction of flagellar rotation. *Proc Natl Acad Sci USA* **85**: 6711–6715.

Zhao, R., Schuster, S.C., and Khan, S. (1995) Structural effects of mutations in *Salmonella typhimurium* flagellar switch complex. *J Mol Biol* **251**: 400–412.

Zhao, R., Amsler, C.D., Matsumura, P., and Khan, S. (1996) FliG and FliM distribution in the *Salmonella typhimurium* cell and flagellar basal bodies. *J Bacteriol* **178**: 258–265.